Journal of the Serbian Chemical Society
JSCS-info@shd.org.rs • www.shd.org.rs/JSCS
J. Serb. Chem. Soc. *85* (6) 795–807 (2020)
JSCS–5339
UDC 546.56+621.352:544.654.2:537.3
Original scientific paper

Copper deposits obtained by pulsating overpotential regime with a long pause and pulse duration from sulfate solutions

FATEMEH K. T. SHAFIEI[1], KOUROSH JAFARZADEH[1]* and ALI REZA MADRAM[2]

[1]*Faculty of Materials Engineering. Malek-Ashtar University of Technology, Tehran, Iran and*
[2]*Faculty of Chemical Engineering. Malek-Ashtar University of Technology, Tehran, Iran*

(Received 12 July, revised 18 October, accepted 12 November 2019)

Abstract: The morphologies of the copper deposits obtained by pulsating overpotential regime with prolonged pulse and pause durations from the solution of 0.15 M $CuSO_4$ in 0.50 M H_2SO_4 at overpotentials lower, higher and belonging to the plateau of limiting diffusion current density were compared with those obtained by the same electrodeposition regime from solutions of 0.075 and 0.30 M $CuSO_4$ in 0.50 M H_2SO_4 and 0.15 M $CuSO_4$ in 0.25 and 1.00 M H_2SO_4 at overpotentials outside the plateau of limiting diffusion current density. These samples were characterized by scanning electron microscopic (SEM) analysis and the cathodic polarization characteristics from solutions compared. Increasing the Cu(II) concentration led to an increase in the limiting diffusion current density. Decreasing the H_2SO_4 concentration shifts both beginning and the end of the plateau of the limiting diffusion current density towards higher electrodeposition overpotentials. Also, electrodeposition in solutions of 0.15 M $CuSO_4$ in 0.25 and 1.00 M H_2SO_4 led to the formation of morphological forms of copper deposits characteristic for electrodeposition of copper from higher $CuSO_4$ or lower H_2SO_4 in solution at some higher overpotentials.

Keywords: electrodeposition; pulsating overpotential; morphology; copper.

INTRODUCTION

The open porous structures with the extremely high surface area are ideally suited for many electrochemical devices, such as batteries, fuel cells, sensors, capacitors as well as for catalytic purpose and can be formed by a very suitable way named electrodeposition.[1–7] Morphological characteristic are probably the most important property of the electrodeposited metal. It depends mainly on the kinetic parameters of the deposition process, current density, overpotential which affect the grain size, nucleation and growth rate of the deposit.[8] In the real condition, the size and shape of powder particles depend on electrolysis regime,

* Corresponding author. E-mail: kjafarzadeh@mut.ac.ir
https://doi.org/10.2298/JSC190712128S

solution composition, deposition time, temperature, hydrodynamic regime, cathodic material and *etc.*[9]

During the electrodeposition, the hydrogen gas evolution is a troublesome process and can adversely affect the metal coating quality.[10] These H_2 bubbles are used as a dynamic template to create a wide range of porous metal films.[5] Templating mechanism and hydrogen bubble behavior on the morphology of porous copper foams have been reported.[11,12] Open and porous copper deposits formation by the regimes of the pulsating current,[13–15] pulsating overpotential,[16] electrodeposition at galvanostatic[17] and potentiostatic[15,18] modes have been the subject of many investigations. In pulsating electrodeposition, the potential or current is alternated between two different values and cause the ions easier passage through negatively charged layer around the cathode.[19]

The most often employed electrolytes for the electrodeposition of copper are those based on aqueous solutions of sulfuric acid and cupric sulfate.[20] Ionic equilibrium calculation of copper electrodeposition electrolytes species over a wide range of concentrations and temperatures was shown by Pinter's model. Increasing the copper concentration produces a sharp decrease in the hydrogen ion concentration while increasing the concentration of sulfuric acid produces an increase in the hydrogen ion concentration.[21] The effect of different concentrations of copper (II) ions and overpotentials on the critical conditions for the formation of the honey-comb structure were determined in the copper electrodeposition processes.[22] The copper deposits obtained by different square-waves pulsating overpotential from 0.15 M $CuSO_4$ in 0.50 M H_2SO_4 were compared with those obtained by potentiostatic electrodeposition (1000 mV) from both 0.075 and 0.30 M $CuSO_4$ in 0.50 M H_2SO_4. It was shown that the effect of decreasing deposition pulse was equivalent to the increasing $CuSO_4$ concentration while the effect of the decreasing pause duration was equivalent to increase of H_2SO_4 concentration in the constant regime.[16] Morphology of deposits obtained by constant overpotential electrodeposition in the hydrogen co-deposition range from six solutions with different concentration of $CuSO_4$ and H_2SO_4 were compared with those formed by the square-waves pulsating current with different pause to pulse ratio.[14] It was found that with increasing the hydrogen ion and copper concentration, the nuclei size increased while the nuclei population density decreased. An increase in the deposition potential produced smaller nuclei size and higher nuclei population density.[23]

However, in spite of investigation of copper deposits structures obtained at high overpotentials in the constant regime and pulsating overpotential regime with prolonged pause duration,[18] the effect of prolonged pulse and pause durations in pulsating overpotential regime on copper electrodeposition from the solutions with different concentrations of sulfuric acid and cupric sulfate is not explored. For this reason, our investigation aimed to examine copper deposited

morphologies by utilizing SEM to provide the correlation between the morphological information and H_2SO_4 and $CuSO_4$ concentrations on the prolonged both pulse and pause in pulsating electrodeposition of copper at cathodic overpotentials outside the plateau of the limiting diffusion current density.

EXPERIMENTAL

The cathodic polarization curves for electrodeposition of copper were recorded potentiostatically by changing the overpotential in 5 mV steps from the following solutions:

a) 0.15 M $CuSO_4$ + 0.50 M H_2SO_4; solution (I)
b) 0.075 M $CuSO_4$ + 0.50 M H_2SO_4; solution (II)
c) 0.30 M $CuSO_4$ + 0.50 M H_2SO_4; solution (III)
d) 0.15 M $CuSO_4$ + 0.25 M H_2SO_4; solution (IV) and
e) 0.15 M $CuSO_4$ + 1.00 M H_2SO_4; solution (V)

Square-wave pulsating overpotential technique was used for copper film electrodeposition from these solutions on the high purity copper (99.8% Cu) foil as the working electrode. Electrodeposition was performed in a three-electrode experimental open cell with Pt grid auxiliary electrode and Ag/AgCl (3 M KCl) as reference electrode at a temperature of 18.0±1.0 °C. The geometric surface area of the working electrodes was 4.7 cm^2. The distance between the working and the counter electrode was 1 cm. In all experiments, constant pulse and pause durations were 30 and 100 ms, respectively. The deposition time was 480 s and the overpotential amplitudes at which copper was electrodeposited from all solutions were: 1100, 1250, 1400 and 2000 mV. The overpotential amplitude values for deposition from solution (I) were selected to be 200, 500 and 800 mV. After electrodeposition, copper deposits were immediately rinsed in distilled water and acetone then dried by the warm air flow. SEM microphotographs corresponding to morphologies of copper deposits obtained at desired overpotential amplitudes were characterized using a Tescan Digital microscopy. Energy dispersive microanalysis (EDS) of deposits at desired overpotential amplitudes were performed during SEM measurements. Double distilled water and analytical grade chemicals were used for the preparation of the solutions for polarization curve record and electrodeposition of copper. All experiments were performed by Autolab (GTSTAT101).

RESULTS AND DISCUSSION

The polarization curves for the electrodeposition of copper from all solutions with well-defined plateaus of the limiting diffusion current density as the typical representatives of the group of intermediate metals are given in Fig. 1. Each curve was swept from the zero potential into more negative potentials with the scan rate of 5 mV s^{-1}.

The polarization curves consisted of three parts. The first linear part of the dependence of the current density on overpotential is the activation control. After the inflection point, the end of the plateau is determined as the overpotential at which current density started to grow with the increasing overpotential.[22] This rapid grow is due to the hydrogen evolution as a parallel reaction.[24,25] As can be seen from Fig. 1, decreasing the Cu(II) concentration leads to the decrease of the limiting diffusion current density, as well as shifting of both the beginning and the end of the plateau of the limiting diffusion current density towards lower

deposition overpotentials. This can be explained by Nernst limiting current density:

$$j_L = nFDc_0/\delta \quad (1)$$

where j_L is the limiting diffusion current density, D is the diffusion coefficient, nF is the number of Faradays per mole of consumed ions, c_0 is the concentration of Cu(II) ions and δ is the thickness of the diffusion layer. Therefore, a change of the Cu(II) concentration of the solution affects the limiting diffusion current density. Increasing the depositable Cu(II) ions in the cathode diffusion layer leads to decrease the concentration type of polarization.[26] As can be seen from Fig. 1, with the decreasing concentration of H_2SO_4, the beginning of the plateau of the limiting diffusion current density was slightly shifted to higher electrodeposition overpotentials. The small shifting of the end of the plateau of the limiting diffusion current density to lower overpotentials can be neglected.[25] Morphologies of copper deposited by pulsating overpotential regime from solutions (I) and (II) at overpotential amplitudes of 1100, 1250, 1400 and 2000 mV are presented in Figs. 2 and 3, respectively.

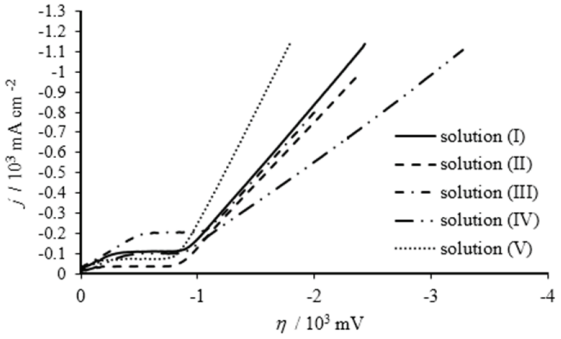

Fig. 1. Polarization curves for the cathodic process of copper deposition from the solutions.

Copper dendrites obtained at the overpotential amplitude of 1400 mV (Figs. 2d and 3d) were more highly branched structures than the ones obtained at the overpotential amplitudes of 1100 and 1250 mV (Figs. 2a and b, and 3a and b). It is well known that the increase in overpotential amplitude leads to the decrease in time needed for the initiation of dendritic growth.[19] Then, further branched dendrites are formed.

Analysis of the copper deposits obtained at the overpotential amplitude of 2000 mV (Fig. 2d–e) shows two types of holes formed due to attached hydrogen bubbles. One type of holes are very similar to those named honeycomb-like structure and the other with a larger diameter are dish-like holes. This structure is very similar to that obtained from 0.30 M $CuSO_4$ in 0.50 M H_2SO_4 during potentiostatic deposition at the overpotential of 1000 mV.[8] Fig. 2f shows copper dendrite formed at the dish-like shoulders.

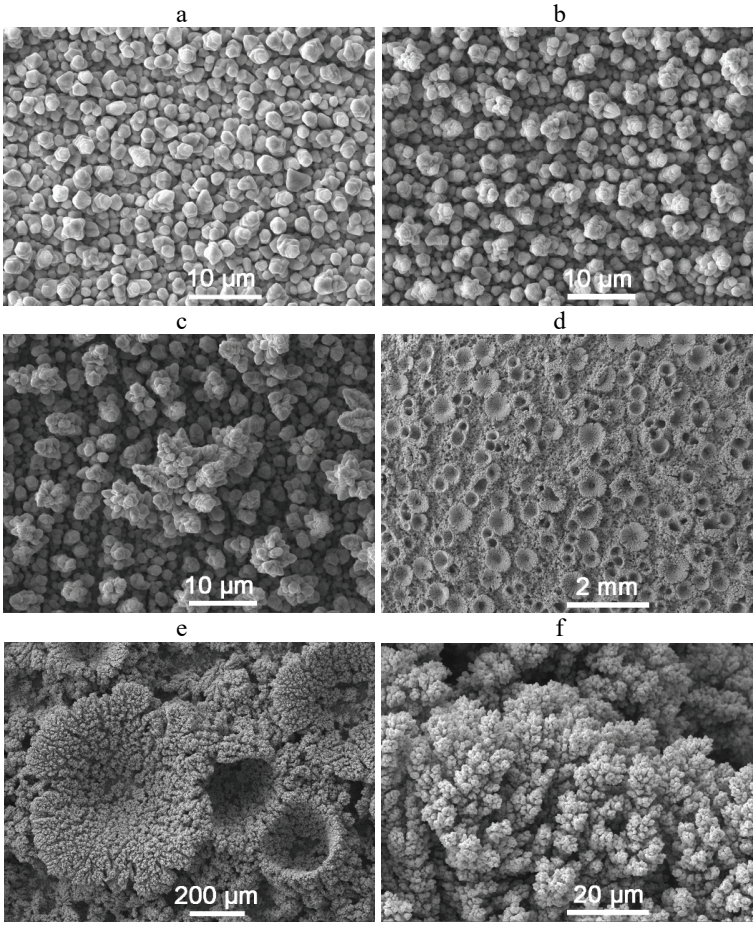

Fig. 2. Morphologies of copper deposits obtained by pulsating overpotential regime from 0.15 M $CuSO_4$ + 0.50 M H_2SO_4 (solution (I)) at overpotential amplitudes of: a) 1100, b) 1250, c) 1400 and d–f) 2000 mV. Pulse duration: 30 ms. Pause duration: 100 ms.

Nikolic *et al*. explained the dish-like hole structures formation. The initial stage of the formation of dish-like holes and the honeycomb-like structure is the same. The number of formed "nuclei" of hydrogen bubbles at active sites on the electrode surface was smaller than the number which led to the formation of the honeycomb-like structure.[8] In the growth process, they have enough space to develop into large bubbles, making holes with a dish-like shape at the surface of the electrode.

The copper morphologies consisted of dendrites, degenerate dendrites and channels (Fig. 3d) obtained by pulsating overpotential at overpotential amplitude of 2000 mV from solution (II), proves that there is no hydrogen evolution or evolved hydrogen is not sufficient to form holes.

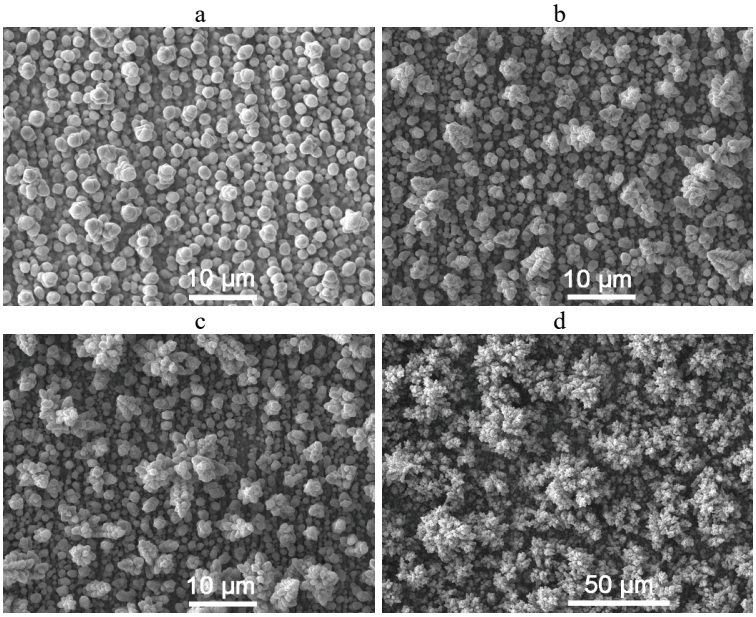

Fig. 3. Morphologies of copper deposits obtained by pulsating overpotential regime from 0.075 M $CuSO_4$ + 0.50 M H_2SO_4 (solution (II)) at overpotential amplitudes of: a) 1100, b) 1250, c) 1400 and d) 2000 mV. Pulse duration: 30 ms. Pause duration: 100 ms.

The change of copper deposit structures during the electrodeposition from solutions (I) and (II) with the increase of electrodeposition overpotential amplitude from 1100 to 2000 mV can be observed in Fig. 4 with further magnification. SEM images show that some grains grow from pyramid-like precursors of dendrites (Fig. 4a) to dendrites (Fig. 4b) and very branchy dendrites (Fig. 4c) or degenerate dendrites (Fig. 4d) by electrodeposition at overpotential amplitudes of 1100, 1250 and 1400 and 2000 mV, respectively.

The deposits size and the optimal value of the dendrite tip decrease with increasing the applied overpotential amplitude.[9] The uniform distribution of morphological forms of copper grains obtained at the overpotential amplitudes of 1100, 1250 and 1400 mV from solutions (III) and (IV) are shown in Fig. 5a–c and 6a–c. The type of electrolyte has a strong effect on the surface morphology.

It can be noticed that a big increase in the copper concentration (solution (III)) or decrease of the sulfuric acid concentration (solution (IV)) lead to a big change in copper deposit morphologies. There is hardly hydrogen evolution as evident from the morphologies in Figs. 5 and 6a–c.

The activity and available sites of hydrogen ions significantly decreased[27] and the obtained copper structures consisted of copper grains. The grains grown by electrodeposition on the initially formed nuclei practically touch each other and there is no new nucleation on already existing grains.[20] The difference in

size between grains can also be observed. This is due to the fact that the nucleation does not occur simultaneously over the whole cathode surface. It is a process extended in time, therefore crystals generated earlier may be considerably larger in the size than ones generated later (Fig. 5a and c).[18,25]

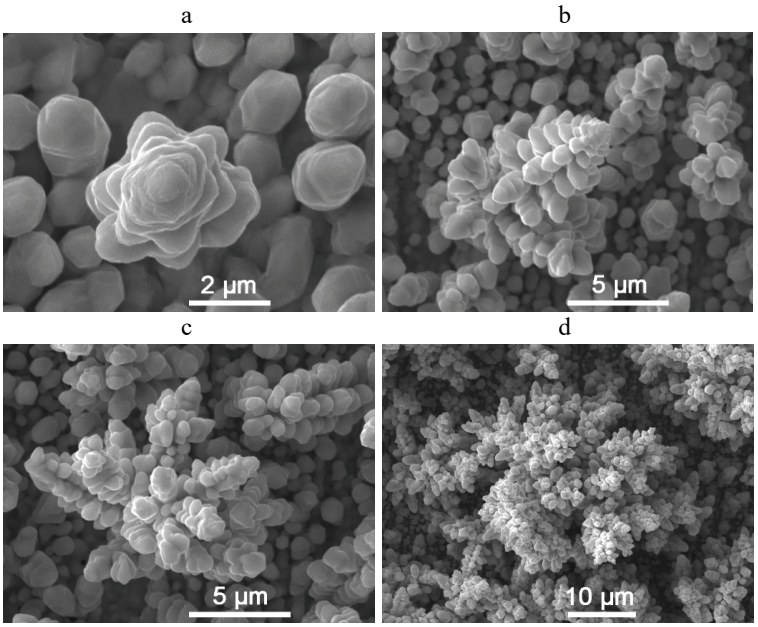

Fig. 4. Deposit structures obtained by pulsating overpotential regime from solutions (I) and (II): a) top view of the pyramid-like precursors of dendrites at 1100 mV, b) dendrites at 1250 mV, c) branchy dendrites at 1400 mV and d) degenerate dendrites at 2000 mV. Pulse duration: 30 ms. Pause duration: 100 ms.

Fig. 5d shows the cauliflower-like agglomerates of grains formed at the potential amplitude of 2000 mV. As shown in Fig. 5e, energy-dispersive spectroscopy (EDS) analysis demonstrated that the foil was successfully covered with pure copper electrodeposited from solution (III) at 1250 mV (Fig. 5b).

Top view of the morphology of copper deposited at an overpotential amplitude of 2000 mV with lower magnification shows a semi dish-like hole, compacted dendritic agglomerates and small dendrites on them (degenerate dendrite) (Fig. 6d).

Morphologies of copper deposits obtained from solution (I) at the lower overpotential amplitudes of (200 mV), inside (500 and 800 mV) the plateau of the limiting diffusion current density is presented in Fig. 7. The careful analysis of the morphologies of the copper deposits shown in Figs. 5–7 indicated that the electrodeposition from solutions (III) and s (IV) at overpotential amplitudes outside the plateau of the limiting diffusion current density (1100, 1250 and 1400

mV) led to the formation of regular, compact and well-dispersed deposits with small grain size (Figs. 5a–c and 6a–c) which are very similar to the deposits formed at overpotential amplitudes at lower and inside the plateau of the limiting diffusion current density (200, 500 and 800 mV) from the solution (I) (Figs. 7a–c).

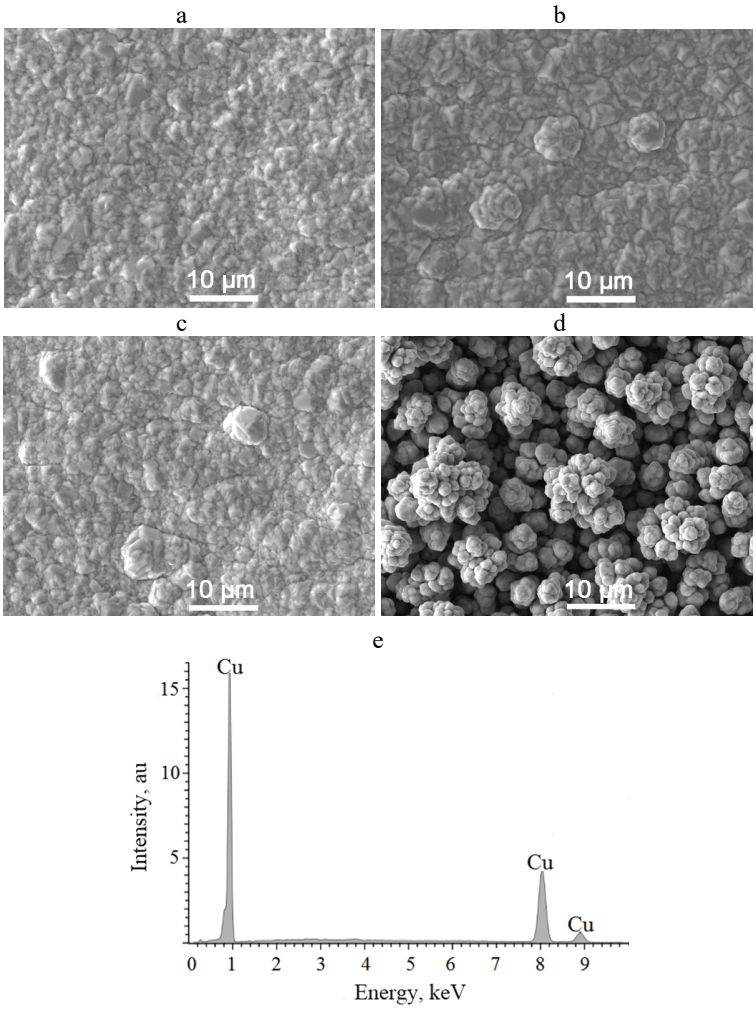

Fig. 5. Morphologies of copper deposits obtained by pulsating overpotential regime from 0.30 M $CuSO_4$ + 0.50 M H_2SO_4 (solution (III)) at overpotential amplitudes of: a) 1100, b) 1250, c) 1400 and d) 2000 mV; e) EDS analysis of the obtained typical copper grain microstructure. Pulse duration: 30 ms. Pause duration: 100 ms.

Fig. 8 shows the copper deposits obtained at overpotential amplitudes of 1100, 1250, 1400 and 2000 mV from solution (V). For the solutions with the concentration of 0.15 M $CuSO_4$, by increasing the acid concentration from 0.25

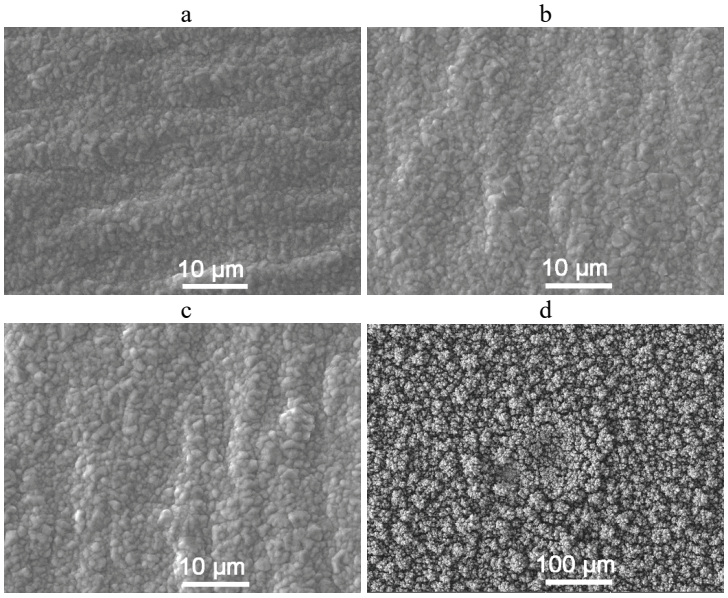

Fig. 6. Morphologies of copper deposits obtained by pulsating overpotential regime from solution 0.15 M $CuSO_4$ + 0.25 M H_2SO_4 (solution (IV)) at overpotential amplitudes of: a) 1100, b) 1250 c) 1400 and 2000 mV. Pulse duration: 30 ms. Pause duration: 100 ms.

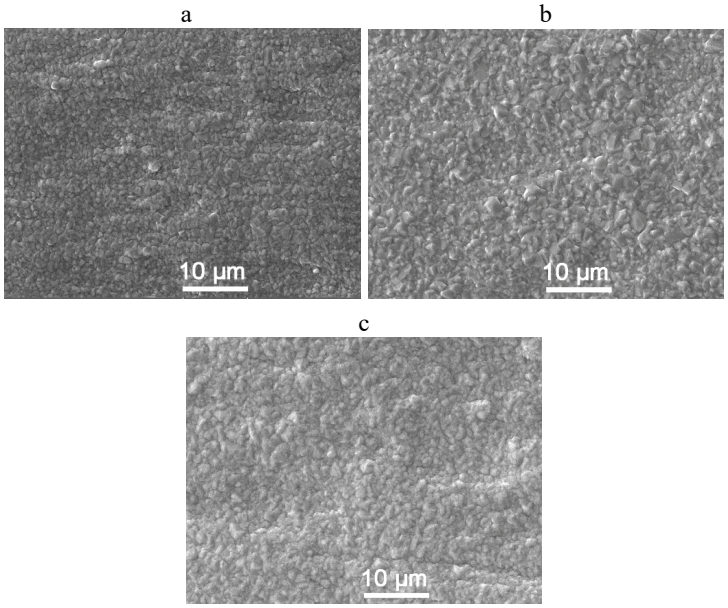

Fig. 7. Morphologies of copper deposits obtained by pulsating overpotential regime from 0.15 M $CuSO_4$ + 0.50 M H_2SO_4 (solution (I)) at overpotential amplitudes of: a) 200, b) 500 and c) 800 mV. Pulse duration: 30 ms. Pause duration: 100 ms.

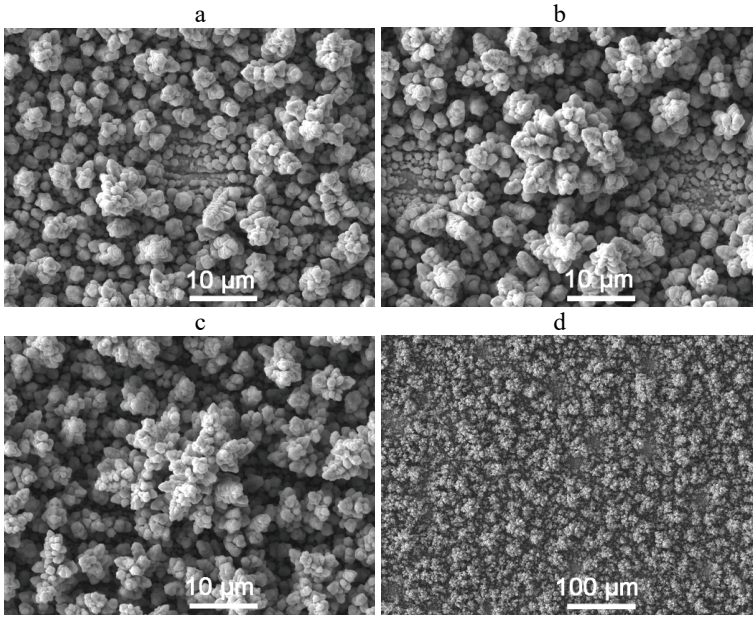

Fig. 8. Morphologies of copper deposits by pulsating overpotential regime from 0.15 M $CuSO_4$ + 1.00 M H_2SO_4 ((V)) at overpotential amplitudes of: a) 1100, b) 1250 and c) 1400 and 2000 mV. Pulse duration: 30 ms. Pause duration: 100 ms.

(solution (IV)) to 0.50 (solution (I)) and 1.00 M (solution (V)), the morphology changes from compact grains (Fig. 6) and dendrite (Fig. 2) to dendrite and hole structure (Fig. 8a, b and d). Increasing the acid concentration led to a higher rate of hydrogen evolution and consequently to hydrogen bubbles production. Adsorption of the hydrogen bubbles on the surface generates the holes.

The appearance of dendritic forms indicates a decreased effectiveness of the stirring of the copper solution by the evolved hydrogen with prolonged pause duration.[28] The prolongation of deposition pulse duration led to the increase of both the rate of hydrogen evolution and copper electrodeposition. The number of hydrogen bubbles formed depends on the overpotential amplitude. Even though the overpotential amplitudes of 1100, 1250 and 1400 and 2000 mV corresponding to the outside the plateau of the limiting diffusion current density were used, holes originating from the attached hydrogen bubbles were not formed.[29]

The low number or absence of holes indicated that the deposition pause of 100 ms is too long to produce sufficient hydrogen to change the hydrodynamic conditions in the near-electrode layer which led to the formation of open and porous honeycomb-like structures. The proof of this are branched dendrites (Fig. 8c) and rare holes (Fig. 8a,b and d) formed on the electrode surface.[30] Hydrogen bubbles detachment formed the individual holes.[31] Dendritic copper agglomerates are well- dispersed and surrounded by irregular channels as shown in Fig. 8d

as well as in Figs. 6d and 3d, show the typical cauliflower-like agglomerates of copper dendrites obtained by the square-wave pulsating overpotential at overpotential amplitude of 2000 mV with the prolonged deposition pulse and pause of 30 and 100 ms, respectively.

CONCLUSION

The effect of concentrations of copper sulfate and sulfuric acid on the copper electrodeposited by pulsating overpotential regime with a prolonged pulse and pause durations at overpotentials outside the plateau of the limiting diffusion current density was examined. By analyzing the morphological characteristics of the copper deposits the results were obtained on the pulsating electrodeposition.

The copper grains obtained from the copper solutions containing 0.30 M $CuSO_4$ in 0.50 M H_2SO_4 (solution(III)) and 0.15 M $CuSO_4$ in 0.25 M H_2SO_4 (solution (IV)) at overpotentials amplitudes values outside the plateau of the limiting diffusion current density (1100, 1250 and 1400 mV) are very similar to the deposits obtained from the solution containing 0.15 M $CuSO_4$ in 0.50 M H_2SO_4 (solution (I)) at overpotential amplitudes belonging to the plateau of the limiting diffusion current density and lower (200, 500 and 800 mV).

A very long pause duration suppresses the hydrogen evolution reaction. Only in two cases dish-like holes were obtained: from 0.15 M $CuSO_4$ in 0.50 M H_2SO_4 (solution (I)) and 0.15 M $CuSO_4$ in 1.00 M H_2SO_4 (solution (III)) at high overpotential amplitude of 2000 mV. Although the potentials outside the plateau of the limiting diffusion current density were used, no honeycomb structure was created in any of the solutions.

Acknowledgement. The authors are grateful to Dr. N. D. Nikolic (ICTM – Department of Electrochemistry, University of Belgrade) for his encouragement and helpful discussions during the preparation of this paper.

ИЗВОД

ТАЛОЗИ БАКРА ДОБИЈЕНИ ИЗ СУЛФАТНИХ РАСТВОРА У РЕЖИМУ ПУЛСИРАЈУЋЕ ПРЕНАПЕТОСТИ СА ДУГОМ ПАУЗОМ И ДУГИМ ПУЛСОМ

FATEMEH K. T. SHAFIEI[1], KOUROSH JAFARZADEH[1] и ALI REZA MADRAM[2]

[1]*Faculty of Materials Engineering. Malek-Ashtar University of Technology, Tehran, Iran u* [2]*Faculty of Chemical Engineering. Malek-Ashtar University of Technology, Tehran, Iran*

Направљено је поређење морфологија талога бакра добијених из раствора 0,15 M $CuSO_4$ у 0,50 M H_2SO_4 у режиму пулсирајуће пренапетости са продуженим трајањем пулса и паузе на пренапетостима које одговарају граничној дифузионој струји, као и вишим и нижим у односу на ту вредност, са талозима добијеним из раствора 0,075 и 0,30 M $CuSO_4$ у 0,50 M H_2SO_4 и раствора 0,15 M $CuSO_4$ у 0,25 и 1,00 M H_2SO_4 у истом режиму таложења на пренапетостима изван платоа граничне дифузионе густине струје. Узорци су карактерисани скенирајућом електронском микроскопијом. Упоређене су и поларизационе криве таложења бакра из наведених раствора. Повећање концентрације јона Cu(II) је довело до повећања граничне дифузионе густине струје. Смањење концентрације H_2SO_4 померило је почетак и завршетак платоа граничне дифузионе струје ка

вишим пренапетостима. Такође, електрохемијским таложењем из раствора 0,15 M $CuSO_4$ у 0,25 и 1,00 M H_2SO_4 формирани су талози чија је морфологија карактеристична за таложење из раствора веће концентрације $CuSO_4$ или мање концентрације H_2SO_4 при вишим пренапетостима.

(Примљено 12. јула, ревидирано 18. октобра, прихваћено 12. новембра 2019)

REFERENCES

1. H.-C. Shin, J. Dong, M. Liu, *Adv. Mater*. **15** (19) (2003) 1610 (http//doi.org/10.1002/adma.20030516)
2. D. H. Nam, R. H. Kim, D. W. Han, H. S. Kwon, *Electrochim. Acta* **66** (2012) 126 (https://dx.doi.org/10.1016/j.electacta.2012.01.084)
3. S. Eugenio, T. M. Silva, M. J. Carmezim, R. G. Duarte, M. F. Montemor, *J. Appl. Electrochem.* **44** (2014) 455 (https://dx.doi.org/10.1007/s10800-013-0646-y)
4. T. N. Huan, Ph. Simon, G. Rousse, I. Genois, V. Artero, M. Fontecave, *Chem. Sci*. **8** (2017) 742 (https://dx.doi.org/10.1039/c6sc03194c)
5. B. J. Plowman, L. A. Jones, S. K. Bhargava, *Chem. Commun*. **51** (2015) 4331 (https://dx.doi.org/10.1039/c4cc06638c)
6. H. Singh, P. B. Dheeraj, Y. P. Singh, G. Rathore, M. Bhardwaj, *J. Electroanal. Chem*. **785** (2017) 1 (https://dx.doi.org/10.1016/j.jelechem.2016.12.013)
7. Y. Li, W-Z. Jia, Y-Y. Song, X-H. Xia, *Chem. Mater.* **19** (2007) 5758 (https://dx.doi.org/10.1021/cm071738j)
8. N. D. Nikolic, Lj. J. Pavolic, M. G. Pavolic, K. I. Popov, *Electrochem. Acta* **52** (2007) 8096 (https://dx.doi.org/10.1016/j.electacta.2007.07.008)
9. K. I. Popov, S. S. Djokic, N. D. Nikolic, V. D. Jovic, *Electrodeposited Alloy Powders, Morphology of Electrochemically and Chemically Deposited Metals*, Springer, Basel, 2016, p. 291 (https://dx.doi.org/10.1007/978-3-319-26073-0_8)
10. W. L. Tasi, P. C. Hsu, Y. Hwu, C. H. Chen, L. W. Chang, J. H. Je, H. M. Lins, A. Groso, G. Margaritondo, *Nature* **417** (2002) 139 (https://dx.doi.org/10.1038/417139a)
11. H. Zhang, Y. Ye, R. Shen, C. Ru, Y. Hu, *J. Electrochem. Soc*. **160** (2013) D441 (https://doi.org/10.1149/2.019310jes)
12. W. Zhang, C. Ding, A. Wang, Y. Zeng, *J. Electrochem. Soc*. **162** (2015) D365 (https://dx.doi.org/10.1149/2.0591508jes)
13. N. D. Nikolic, G. Brankovic, K. I. Popova, *Mater. Chem. Phys*. **125** (2011) 587 (https://doi.org/10.1016/j.elecom.2010.03.021)
14. N. D. Nikolic, G. Brankovic*, Electrochem. Commun*. **12** (2010) 740 (https://dx.doi.org/10.1016/j.elecom.2010.03.021)
15. N. D. Nikolic, Lj. J. Pavlovic, S. B. Kristic, M. G. Pavlovic, K. I. Popov, *Chem. Eng. Sci*. **63** (2008) 2824 (https://dx.doi.org/10.1016/j.ces.2008.02.022)
16. N. D. Nikolic, G. Brankovic, M. G. Pavlovic, *Powder Techol*. **221** (2012) 271(https://dx.doi.org/10.1016/j.powtec.2012.01.014)
17. N. D. Nikolic, G. Brankovic, *Mater. Lett*. **70** (2012) 11 (https://dx.doi.org/10.1016/j.matlet.2011.11.081)
18. N. D. Nikolic, K. I. Popov, Lj. J. Pavlovic, M. G. Pavlovic, *Surface Coat. Technol*. **201** (2006) 560 (https://dx.doi.org/10.1016/j.surfcoat.2005.12.004)
19. M. S. Chandrasekar, M. Pushpavanam, *Electrochim. Acta* **53** (2008) 3313 (https://dx.doi.org/10.1016/j.electacta.2007.11.054)
20. F. A. Lowenheim, Electroplating, McGraw-Hill Book Company, New York, 1978
21. N. D. Nikolic, , *Zaštita materijala* **51** (2010) 197

22. N. D. Nikolic, K. I. Popov, Lj. J. Pavlovic, M. G. Pavlovic, *Sensors* **7** (2007) 1 (https://dx.doi.org/10.3390/s7010001)
23. D. Grujicic, B. Pesic, *Electrochim. Acta* **47** (2002) 2901 (https://dx.doi.org/10.1016/s0013-4686(02)00161-5)
24. K. I. Popov, P. M. Zivkovic, B. Jokic, N. D. Nikolic*, J. Serb. Chem. Soc.* **81** (2016) 291 (https://dx.doi.org/10.2298/jsc150717076p)
25. N. D. Nikolic, K. I. Popov*, Hydrogen co-deposition effects on the structure of electrodeposited copper, Modern Aspects of Electrochemistry*, S. S. Djokic, Ed., Springer-Verlag, New York, 2010, p. 1 (https://dx.doi.org/10.1007/978-1-4419-5589-0_1)
26. M. M. Kamel, A. A. El-Moemen, S. M. Rashwan, A. M. Bolbol, *Metals* **6** (2017) 179
27. J. M. Casas, F. Alvarez, L. Cifuentes, *Chem. Eng. Sci*. **55** (2000) 6223 (https://dx.doi.org/10.1016/s0009-2509(00)00421-8)
28. N. D. Nikolic, V. M. Maksimovic, M. G. Pavlovic, K. Popov*, J. Serb. Chem. Soc*. **74** (2009) 689 (https://dx.doi.org/10.2298/jsc0906689n)
29. N. D. Nikolic, G. Brankovic, V. Maksimovic, *J. Electoanal. Chem*. **635** (2009) 111 (https://dx.doi.org/10.1016/j.jelechem.2009.08.005)
30. L. Avramovic, V. M. Maksimovic, Z. Bascarevic, N. Ignjatovic, M. Bugarin, R. Markovic, N. D. Nikolic, *Metals* **9** (2019) 2 (https://dx.doi.org/10.3390/met9010056)
31. N. D. Nikolic, P. M. Zivkovic, B. Jokic, M. G. Pavlovi, J. S. Stevanovci, *Maced. J. Chem. Chem. Eng.* **33** (2014)169 (https://dx.doi.org/10.20450/mjcce.2014.509).